Received: 4 July 2020 | Accepted: 15 July 2020

DOI: 10.1002/cav.1940

SPECIAL ISSUE PAPER

WILEY

Real-time suturing simulation for virtual reality medical training

Peng Yu[1,2] | **Junjun Pan**[1,2,3] | **Hong Qin**[4] | **Aimin Hao**[1,2] | **Haipeng Wang**[5]

[1]State Key Laboratory of Virtual Reality Technology & Systems, Beihang University, Beijing, China

[2]Peng Cheng Lab, Shenzhen, China

[3]Faculty of Media and Communication Bournemouth University, Dorset, UK

[4]Department of Computer Science, State University of New York at Stony Brook, New York, New York,

[5]Beijing Aerospace General Hospital, Beijing, China

Correspondence
Junjun Pan, State Key Laboratory of Virtual Reality Technology & Systems, Beihang University, Beijing, China.
Email: pan_junjun@buaa.edu.cn
Hong Qin, Department of Computer Science, State University of New York at Stony Brook, New York, NY.
Email: qin@cs.stonybrook.edu

Abstract

At present, virtual reality (VR) -based medical simulators provide an efficient and cost-effective alternative without exposing risk to the traditional training approaches. As an essential and indispensable task in fundamental surgical skills training, the research of suturing simulation still remains insufficient in the field of virtual surgery. In this paper, we present a real-time suturing simulation framework which can handle the complex interactions between surgical instruments and soft tissue. The simulation consists of two stages: external interaction and internal coupling. External interaction involves the interplay between needle/suture and the soft tissue, which are both deformed by position-based dynamics (PBD) with different constraints. At the internal coupling stage, once the force exceeds a threshold, the needle tip will puncture and penetrate into the soft tissue and generate a path. To guarantee the needle/suture accurately following the path inside the soft tissue, we propose a novel coupling method by matching and generating the constraints among needle, suture, and penetration path. We have applied this suturing simulation into a VR laparoscopic surgery simulator with haptic force. Our experimental results demonstrate that our approach can achieve real-time performance with a high degree of visual realism and haptic fidelity.

KEYWORDS

suturing simulation, position-based dynamics, virtual surgery simulator

1 | INTRODUCTION

According to Reference 1, VR medical simulator provides doctors an intuitive and realistic way of learning surgical skills. It improves surgeons' performance in the operation room and significantly shortens their learning curves. Suturing is a common and indispensable step for almost all the trauma treatment in the clinic. However, most researches in suturing simulation[2-4] focus on the force–displacement measurements and analysis of the flexible needle insertion or the interactions between the rigid needle and soft tissue without considering surgical threads. Though the deformation of soft bodies, the motion of rigid bodies and strands (such as rod, hair, wire etc.) are well investigated in computer graphics, the research in the simulation of the completed suturing process is insufficient due to the technical difficulties. Generally, there are two challenges: One is how to determine whether the needle tip penetrates the soft tissue and how to generate the paths of the needle. The other is how to handle the complex coupling between needle/suture and soft tissue before/after puncture occurs.

In this paper, we present a real-time simulation framework to handle the complex interactions between surgical instruments (needle and suture) and soft tissue in the entire suturing process. There are two research topics: One is the interactions between the needle/suture and the soft tissue mesh. The whole process requires fast and frequent collision detection and response. Another is the coupling for the physical deformation of needle/suture and soft tissue. To address these issues, we divide the suturing procedure into two stages: external interaction and internal coupling. At the first stage, needle/suture, and soft tissue are simulated with independent models. At the external stage, needle and suture are not allowed to puncture into the soft tissue. When the force of needle tip on soft tissue surface goes beyond a threshold, the simulation enters into the internal stage, in which the needle will insert into soft tissue and a path would be generated. During suturing, the rest part of the needle and suture will follow this path. To accurately simulate this process, we propose a novel coupling method to deal with the internal interactions between the needle/suture and soft tissue. In the end, we applied our technique to a VR-based laparoscopic surgery simulator with haptic devices. It can be widely applied to many complex virtual surgery environments. The innovative contributions in this paper can be summarized as follows:

- We present a completed suturing simulation framework, which consists of two stages (external and internal). At the external stage, needle/suture cannot be punctured into the soft tissue but can drive soft tissue deforming. At the internal stage, the needle can insert the soft tissue and generate a path when its force exceeds a threshold.
- We propose a novel coupling method to ensure needle and suture passing through the puncturing path correctly. The coupling constraints are designed to guarantee needle/suture follow the path during motion.
- Finally, we integrate our suturing simulation technique into a VR laparoscopic surgery simulator with haptic feedback. For surgical skills training, users can control haptic devices to suture an open wound.

2 | RELATED WORK

Suturing is a complex procedure that involves the deformation of soft tissue, the motion of needle and suture, and interaction among them. Here we just list the most relevant work.

In the last three decades, soft body deformation has been widely investigated since Terzopoulos et al.[5] introduced the Finite Element Method (FEM) into computer graphics. At present, extensive research has been conducted to employ FEM for simulating deformable objects.[6] FEM is physically accurate and capable of dealing with complex geometry but not suitable for real-time simulation, due to its intensive computation cost. As an alternative, Bender et al.[7] exploited continuum-based formulation to construct the potential energy as position-based dynamics (PBD) constraints of deformable objects. It can perform complex physical effects. In our study, we employ the same manner to handle soft tissue deformation.

The simulation of the strand is another important issue in suturing training. Pai et al.[8] introduced a discretized Cosserat rod model to simulate sutures and catheters in virtual surgery. But it is difficult to handle collision detection due to the implicit representation of strand centerlines. And their models are difficult to integrate into the PBD framework. Kugelstadt et al.[9] and Soler et al.,[10] who treated the orientation in the same manner of positions within PBD framework. However, these models are not fully investigated in suturing simulation, which involves strong and complex coupling between soft tissue. In this paper, needle and suture are all referred to as strands.

To measure the relationship between force and displacement during needle insertion, DiMaio et al.[2] employed a robotic manipulator to insert an elastostatic tissue and used two-dimensional (2D) FEM to simulate needle insertion procedure which is extended to three-dimensional (3D) case in Reference 11. They focus on suture automation rather than simulation and modeling of soft tissue and surgical suture. Chentanez et al.[12] proposed an interactive needle insertion simulator which coupling the steerable needle with deformable tissue. While, most suturing procedures require a rigid needle. Qi et al.[13] proposed a virtual interactive suturing simulation in which Penrose drain is a 2D spring mesh embedded in the 3D model. Nonetheless, Their proposed suturing model can only be applied in limited surgery scenes on account of the lacking volumetric behavior of soft tissue. Xu et al.[14] proposed an inextensible strand model based on Reference 9. A simple suturing experiment was conducted, using intensive spheres to handle collision detection. Nonetheless, the suturing simulation in their paper is just an expedient to show the inextensible of their thread model. And they just apply an oversimplified edge-edge collision detection approach to deal with the interaction between surgical thread and soft tissue.

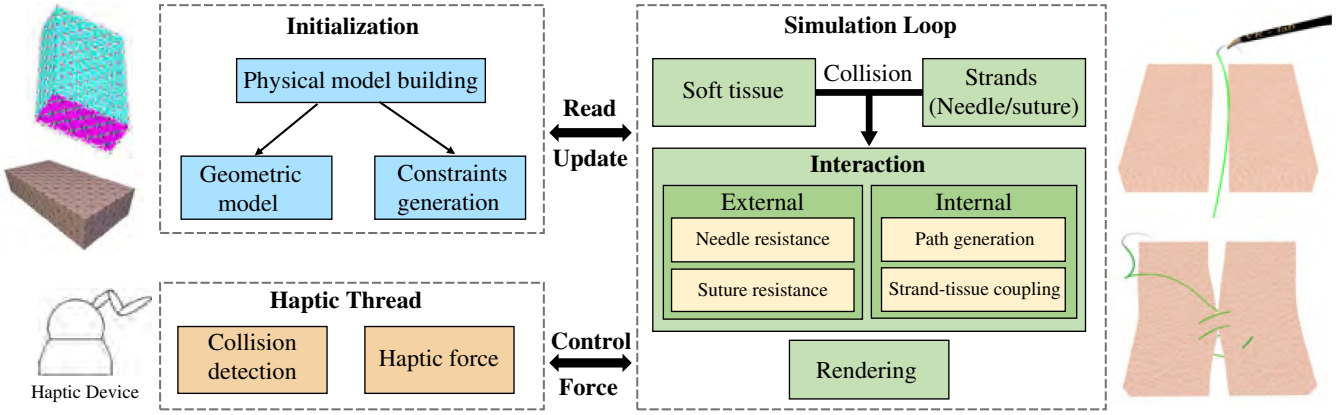

FIGURE 1 The framework of suturing simulation

3 | OVERVIEW

Our suturing framework has three major components (Figure 1). The first is the initialization. We employ tetrahedral mesh and connected particles as our physical model for soft tissue and strands (needle, suture), respectively. Then the relevant constraints are generated to handle the soft tissue deformation and the motion of the strand model. Our interaction algorithm is independent of the physical model of soft tissue and strand. Different kinds of simulation models of soft tissue and strands can be integrated into our suturing simulation framework. The second component is the simulation loop in which constraints the deformation of soft tissue and strands. The collision between strands and soft tissue is handled by our interaction method. During suturing, to obtain realistic force feedback from haptic devices, the third module computes the haptic forces when a collision happens. And the haptic force is transferred to the simulation loop to control the surgical needle.

Our simulation loop is under the PBD framework that contains three steps. Firstly, we use the semi-implicit Euler method to compute predicted positions and orientations for soft tissue and strands. Next, we determine whether the strand has collisions or contacts with soft tissue. If they are intersected, we apply our interaction method in Section 4 to generate corresponding constraints. Secondly, the predicted positions and orientations are iteratively projected to the constraints manifold in Gauss–Seidel fashion. Finally, we use the corrected positions and orientations to update velocities of soft tissue and strands.

4 | INTERACTION BETWEEN SOFT TISSUE AND STRANDS

There are two technical challenges about the interaction strategy between soft tissue and strand. One is how to determine whether the needle tip penetrates soft tissue and where the paths generated by the needle. The other is how to handle the interaction between strands and soft tissue before/after insertion occurs. The first problem is related to our designed suturing framework which separates the whole procedure into two stages: external and internal. To solve the second problem, we establish a new coupling algorithm between the strand and soft tissue.

4.1 | External and internal stages

The major suturing steps are illustrated in Figure 2. To decide whether strand penetrates the soft tissue, we first compute the signed distance field of soft tissue. As shown in Figure 2a, the whole 3D space are divided into three layers: inside (if signed distance $s < 0$), resistance area (if $0 < s < \epsilon$, where ϵ is a threshold), and outside (if $s > \epsilon$). On the surface of soft tissue, the signed distance equal to zero.

As mentioned before, there are two stages during suturing. At the first stage, needle and suture are simulated independently if no intersection occurs. Suture would be projected out of soft tissue using *node-triangle* constraint if the needle tip has not pierced into soft tissue (Figure 2b). If the exerted force of needle head is not large enough, the surface of soft tissue

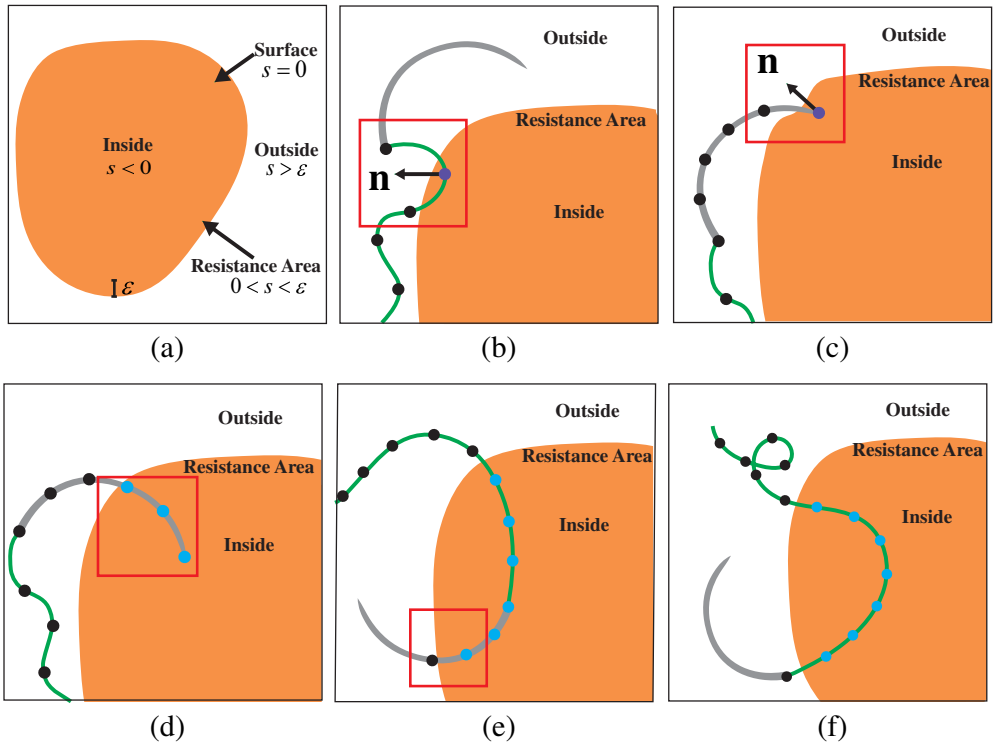

FIGURE 2 Suturing procedure. (a) The signed distance field of soft tissue. External interaction: (b) suture resistance and (c) needle resistance. Internal interaction: (d–f) needle/suture passing through soft tissue. The whole simulation domain is divided into three areas: inside, resistance area, and outside. The color of strand nodes represent types of coupling constraints: black (free nodes), violet (node-triangle constraints) , cyan (node-path constraints).

would resist the insertion of the needle by solving a *node-triangle* constraint as shown in the red square of Figure 2c. At the second stage, if the exerted force exceeds the threshold ε, the needle would pierce through the surface and enter into the inside of soft tissue as Figure 2ds. Then the needle would exit the surface of soft tissue and drag the suture Figure 2e. The following suture can only pass through the access points and path nodes generated by needle head. To pass through access points, we traverse each edge of the strand and create a node-access constraint if the signed distance of both endpoints of this edge is opposite in sign Figure 2f.

The needle tip should be treated differently from the needle body and suture because the needle tip needs to puncture through the soft tissue. Puncturing happens between the needle tip and the tissue surface starts by deforming the tissue at the tissue surface and continues until the contact force reaches its maximum.[3] Besides, if we do not treat them differently, suture could puncture into soft tissue like needle tip. Thus, it is necessary to assign a state for each strand node. Here we assign a state (**HEAD**, **IN**, **OUT**) to each strand node according to their signed distance from the surface of soft tissue. **HEAD** means the strand particle is needle tip, **IN**/**OUT** means the strand (needle body or suture) particle is in/out of the soft tissue.

Meanwhile, computation efficiency is a crucial aspect of VR surgical simulator. To accelerate the simulation, we compute the signed distance and state of strand node through three phases at each time step. Firstly, we compute and update axis-aligned bounding boxes (AABB) of the strand and soft tissue as a broad phase to test whether their boundaries intersect with each other. If they are intersected, kd-trees established before the simulation loop of the strand and soft tissue are traversed with a breadth-first manner. The depth of the tree is near 7–10 levels which can be traversed fast. At last, if any pair of leaves of kd-trees has an intersection, the signed distance field of soft tissue is computed based on the triangle mesh. After computing the signed distance for each strand node, we will update their states, generate a path or path nodes for needle head, and establish new coupling constraints accordingly. When needle tip moves forward, it would pass through the tetrahedra of soft tissue. We store the indices of these tetrahedra and barycentric coordinates of the needle tip in the passed element as a path node. Each path during suturing is composed of a list of path nodes. And Each path is contained in a path vector.

During the suturing procedure, multiple paths and strand segments would be created inside the soft tissue. We should match the strand segments with their corresponding paths at each time step. Fortunately, the order of path and strand segment inside soft tissue are correlative. Generally, the first generated path node matches the first strand segment. We assume that the end of the suture wound not pass through the first created path because the tail end of the suture is usually

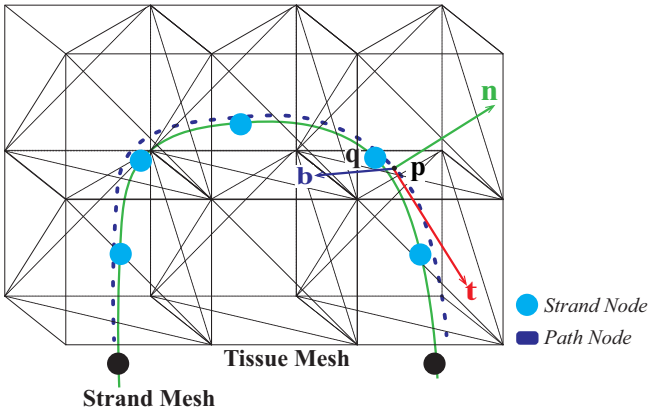

FIGURE 3 Tet-strand coupling. Strand described using the green line is enforced to conform with the path. The cyan strand nodes are coupled with path nodes using node-path constraints

used to tie knots. The newly created path is at the back of the path vector and would match the front strand segments represented using green squares.

4.2 | Coupling of soft tissue and strands

In this section, we will describe the technical details of the *node-path*, *node-triangle*, *node-access*constraints. These constraints are designed to solve the coupling of the strand and soft tissue, when strands pass through the internal path.

Node-path constraint: After matching the strand segments and path, we need to create the coupling constraints between them. For each strand node $\mathbf{q}$ that is inside soft tissue, we find the nearest path node $\mathbf{p}$ from the matched path. According to Reference 12, strand and soft tissue have the same acceleration. The strand can only go along the tangent direction $\mathbf{t}$ of the path (Figure 3). Thus, we could enforce the relative displacement between the strand node and path along the direction orthogonal with tangent $\mathbf{t}$ is zero. We compute the tangent vector based on path nodes, then a node-path constraint can be described as

$$\begin{aligned} C(\mathbf{q}, \mathbf{p}_1, \mathbf{p}_2, \mathbf{p}_3, \mathbf{p}_4) &= \left(\sum_{i=1}^{4} w_i \mathbf{p}_i - \mathbf{q} \right) \times \mathbf{t} \\ &= (\mathbf{p} - \mathbf{q}) \times \mathbf{t} = 0, \end{aligned} \tag{1}$$

where w_i is the component of barycentric coordinates of path node $\mathbf{p}$, $\mathbf{p}_i, i \in [1,4]$ is the ith vertex position of path node's tetrahedron, $\mathbf{t}$ is the tangent vector of the path node. The tangent vector is the arithmetic mean of the path node's adjacent edge vector.

Node-triangle constraint: At the beginning of suturing simulation, the needle tip cannot be inserted into the soft tissue. The user needs to exert enough force on the needle shaft, and then penetrate. In addition, if part of strand falsely entered soft tissue, we project it to the surface. To avoid penetration of a strand nodes, we employ *node-triangle* constraints as

$$C(\mathbf{q}, \mathbf{p}_1, \mathbf{p}_2, \mathbf{p}_3) = (\mathbf{q} - \mathbf{p}_1) \cdot \frac{\mathbf{p}_{21} \times \mathbf{p}_{31}}{\|\mathbf{p}_{21} \times \mathbf{p}_{31}\|} - \varepsilon, \tag{2}$$

where $\mathbf{p}_i, i \in \{1,2,3\}$ is a vertex of triangle, $\mathbf{p}_{ij} = \mathbf{p}_i - \mathbf{p}_j$, $\mathbf{q}$ is a particle of the strand and ε is the threshold. Considering momentum conservation, we take the mass of particles into consideration.

Node-access constraint: At the surface of soft tissue, we use a unique approach to handle the entry and exit of the strands. The strand node might deviate the exit or entrance position, called **access point** in this paper, which is generated when the needle head inserts into or punches out of soft tissue shown in Figure 4. To avert this condition, we need to take care of the boundary condition. All the strand nodes following the needle head node should pass through access points. When the needle head node pass through the surface of soft tissue and its signed distance is lower than the penetration threshold, the triangle on the surface nearest the needle head is stored as an access triangle. The barycentric coordinates of the exit or entrance position of the needle head in the access triangle are stored in a list called access point list. When a

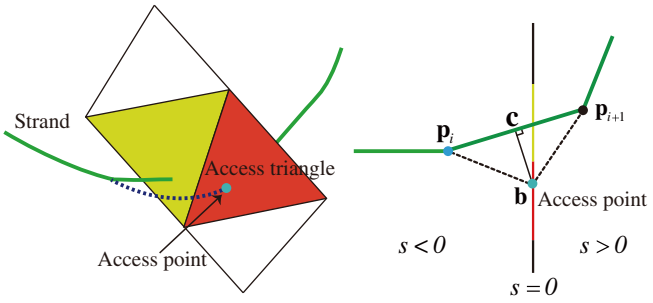

FIGURE 4 Left: strand do not pass through access triangle (red). Right: the black line represents the side view of the soft tissue surface where s is the signed distance. If the segment connected by $\mathbf{p}_i$ and $\mathbf{p}_{i+1}$ does not pass through access triangle which represented as red line, a *node-access constraint* is generated

TABLE 1 Data size and computation efficiency of different models

Model	Tetrahedra	Tets vertices	Triangles	Triangle vertices	Fps
Cubic tissue	6,840	2,000	2,264	6,792	35
Abdominal wall	4,333	1,261	2,308	5,814	38
Abdominal wall (TG)	2,821	869	908	2,724	40
Hand	8,656	2,357	908	2,724	21

segment s_i connected with two strand nodes $\mathbf{p}_i$ and $\mathbf{p}_{i+1}$ pass through the surface of soft tissue shown in Figure 4, a point $\mathbf{c}$ on the segment which is the projection of access point $\mathbf{b}$ would be pulled to access $\mathbf{b}$ to satisfy the constraints that

$$C(\mathbf{p}_i, \mathbf{p}_{i+1}) = \|\mathbf{b} - \mathbf{p}_i\| + \|\mathbf{b} - \mathbf{p}_{i+1}\| - l = 0, \tag{3}$$

where l is the rest length of segment s_i.

4.3 | Path generation

To avoid dense or spare path nodes on the path, we design a generation approach of path node. Our path node generation method ensures that the created path corresponds to strands inside the tissue. In initialization, we set an interval $[l,h]$ of length for two adjacent path nodes. During the forward process of the needle tip, if the distance d_{tp} between the tip and the previous path node is lower than l, the new path node will not be created. When d_{tp} is higher than h, we create $\lfloor d_{tp}/h \rfloor$ path nodes. Otherwise, only one path node will be generated. Basically, we set $l = 1.2cm$, $h = 1.7cm$ in our experiments.

5 | EXPERIMENTAL RESULTS

Our suturing experiments have been implemented using C++ and OpenGL. All experiments were performed on a single core of an Intel(R) Core(TM) i7-7700HQ, 2.8 GHz CPU, 16GB RAM, and NVIDIA Geforce GTX 1070. The tetrahedral mesh of soft tissue is generated using Tetwild. In our experiments, the soft tissue is simulated as an isotropic and homogeneous material. Generally, biological tissue is featured with high damping which results in fast energy dissipation. This damping effect can improve the stability and reduce the oscillation of the particles of an object. Thus, we damped the global motion of all particles by adding a global damping force in terms of velocities.

5.1 | Experiments and comparison

We designed three experiments using the same strand model. Semicircle needle consists of 30 nodes and suture is discretized into 200 nodes. The data size and computation efficiency in three experiments are illustrated in Tables 1 and 2, respectively. Each row of data in Table 2 is the average of ten experiments. In our experiments, Young's modulus and Poisson's rations of soft tissue are 1.0 kPa and 0.5 which are the typical material parameters of soft tissue.

TABLE 2 Computation time of different tasks for three simulation models

Model	Collision detection	Constraints solving	Rendering	Avg. sum time (ms)
Cubic tissue	61.68%	29.12%	4.81%	28.57
Abdominal wall	59.38%	32.49%	5.73%	26.32
Hand	62.14%	31.70%	3.41%	47.62

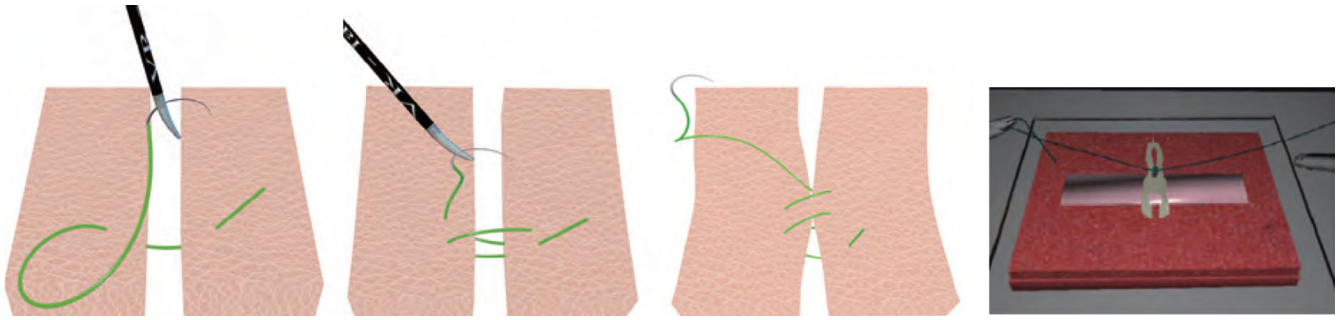

FIGURE 5 Suturing two cubic soft tissue (left three columns), and compared with the result in Reference 13 (the fourth column)

FIGURE 6 Suturing simulation of the abdominal wall

The first experiment is suturing two cubic soft tissue (the left three columns in Figure 5). The particles of both ends of each cube soft tissue are static with the inverse masses equal zeros. We compare its visual performance with the method in Reference 13. Figure 5 (the fourth column) shows the experimental results of Reference 13. The object stitched is a 2D triangle mesh embedded into 3D space. Their method can only simulate the limited virtual surgery scene, which involves simple objects without volumetric deformation. In contrast, our approach could suture open wound on deformable soft tissue which is discretized by tetrahedral mesh. Figure 5 demonstrates the suturing procedure in our simulator. At first, needle controlled by our haptic device penetrates the surface of one cubic soft tissue. Then the needle passes through one cubic soft tissue and penetrates another. The suture is dragged into the soft tissue. Finally, the two elastic bars are stitched together by iteratively operating this procedure.

The second experiment is suturing on an abdominal wall (Figure 6). We also compare our techniques with the methods in Reference 14. In Reference 14, the soft tissue is represented as a mass-spring network, which hardly illustrates the volumetric effects like us. Besides, they apply a different collision detection model. To detect a collision, all of the particles in their scene is simplified with a sphere with radius. When the suture passes through the soft tissue, the edge of the mass-spring is discretized as a series of spheres, which are used to detect the collision and response to the intersection. When the geometry of soft tissue is complex, its method suffers from high computation consumption.

In this experiment, we also try to study the influence of different quality tetrahedral mesh on the simulation performance. In Table 1, two tetrahedral mesh of the abdominal wall model are created by Tetwild (row 2) and Tetgen[15] (row 3) respectively. The max/min ratio of face angle of tetrahedral mesh is 26 and 80, respectively. The quality of the mesh is inversely proportional to the max/min face angle ratio. Though the number of tetrahedra generated by Tetwild is 1.56 times these generated by Tetgen, the simulation speed is almost the same. It is more obvious when comparing the data of the first and third row in Table 1. The number of cube tissue tetrahedra is 2.43 times the abdominal wall (TG) whereas the cube tissue suturing simulation is 0.13 slower than the abdominal wall (TG) suturing. Apart from that, we found that the

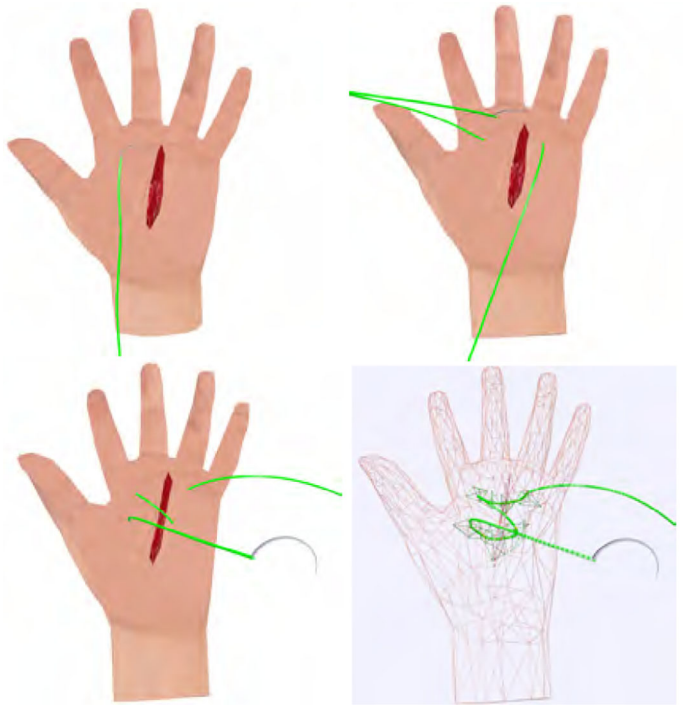

FIGURE 7 Suturing simulation of the hand

bad quality tetrahedral mesh would result in unstable simulation. Therefore, we believe that the quality of the tetrahedral mesh has a strong influence on our suturing simulation technique. The reason is that the discretized mesh is unrelated to the constraints. By using finer and good quality mesh, we can alleviate this problem.

Figure 7 illustrates the suturing process on a hand as the third experiment. We employ Tetgen to generate tetrahedral mesh. However, the max/min ratio of face angle is 100, which means the quality of the volumetric mesh is low. During the suturing process, the simulation may suffer from stability problem. Here Tetwild, which provides better tetrahedral mesh generation, can give a solution.

5.2 | Application and limitations

Our ultimate goal is to apply this novel suturing method in-clinic training for doctors. To validate our techniques, we have incorporated it into a VR laparoscopic surgery simulator (Figure 8) we developed. This prototyped medical simulator has

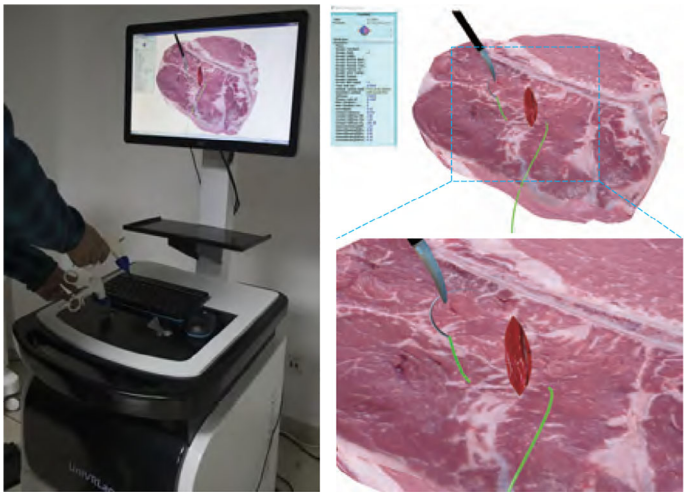

FIGURE 8 Interface of our prototyped virtual reality laparoscopic surgery simulator

been equipped with the fundamental skills functions, such as suturing and cutting, in laparoscopic surgery training. It shows that our suturing simulation can handle the complex scene in real time.

Nevertheless, our approach is not without limitations. As demonstrated in Table 2, the most time-consuming step in our suturing simulation is collision detection. In each time step, we have to regenerate the signed distance field of soft tissue and search the signed distance of each strand node. To ease this problem, we can regenerate the signed distance field when the deformation beyond a threshold. In addition, PBD suffers from physics incorrect artifact which may cause the system energy increasing and iteration/time-step dependent stiffness. We can employ XPBD method[16] to improve the visual performance of Cosserat rod. And we also plan to enforce the inextensibility of strand in our simulator.

6 | CONCLUSION AND FUTURE WORK

This paper presents a real-time simulation framework to handle the complex interactions between strands and soft tissue in suturing. The whole suturing procedure is divided into two stages: external interaction and internal coupling. At the external stage, needle and suture are not allowed to puncture into the soft tissue. It involves the interplay between strands and the soft tissue outside the soft tissue surface. At the internal stage, the needle will insert into soft tissue and a path would be generated. For suturing simulation, we propose a novel coupling method to deal with internal interaction between the suture and soft tissue. Finally, we applied our technique to a VR-based laparoscopic surgery simulator with haptic devices. Experimental results demonstrate that our approach can achieve real-time performance with a high degree of realism and fidelity. Currently, the suturing simulator has not achieved all the suturing steps like knot-typing and self-collision detection of strand and soft bodies. This work is at progress.

ACKNOWLEDGEMENTS

This research is supported in part by National Key R&D Program of China (No. 2018YFC0115102), National Natural Science Foundation of China (No. 61872020, 61532002, 61672149), Beijing Natural Science Foundation Haidian Primitive Innovation Joint Fund (L182016), Beijing Advanced Innovation Center for Biomedical Engineering (ZF138G1714), Research Unit of Virtual Human and Virtual Surgery, Chinese Academy of Medical Sciences' Shenzhen Research Institute of Big Data, Shenzhen 518000.

ORCID

Peng Yu https://orcid.org/0000-0002-8652-2744

REFERENCES

1. Agha RA, Fowler AJ. The role and validity of surgical simulation. Int Surg. 2015;100:350–357.
2. DiMaio SP, Salcudean SE. Simulated interactive needle insertion. Proceedings 10th Symposium on Haptic Interfaces for Virtual Environment and Teleoperator Systems. HAPTICS. Orlando, FL, USA, USA: IEEE; 2002. P. 344–351.
3. Khadem M, Rossa C, Sloboda RS, Usmani N, Tavakoli M. Mechanics of tissue cutting during needle insertion in biological tissue. IEEE Robot Automat Lett. 2016;1:800–807.
4. Jackson RC, Desai V, Castillo JP, Çavuşoğlu MC. Needle-tissue interaction force state estimation for robotic surgical suturing. Proceedings of the 2016 IEEE/RSJ International Conference on Intelligent Robots and Systems. Daejeon, South Korea: IEEE; 2016. p. 3659–3664.
5. Terzopoulos D, Platt J, Barr A, Fleischer K. Elastically deformable models. SIGGRAPH Comput Graph. 1987;21:205–214.
6. Sifakis E, Barbic J. Fem simulation of 3d deformable solids: A practitioner's guide to theory, discretization and model reduction. ACM SIGGRAPH 2012 Courses. Volume 20 Los Angeles, California: ACM, 2012; p. 1–50.
7. Jan Bender, Dan Koschier, Patrick Charrier, and Daniel Weber. Position-based simulation of continuous materials. Comput Graph, 44:1 – 10, 2014.
8. Dinesh KP. Strands: Interactive simulation of thin solids using cosserat models. Comput Graph Forum. 2002;21:347–352.
9. Kugelstadt T, Schömer E. Position and orientation based cosserat rods. Proceedings of the ACM SIGGRAPH/Eurographics Symposium on Computer Animation. Zurich, Switzerland: Eurographics Association; 2016. p. 169–178.
10. Soler C, Martin T, Sorkine-Hornung O. Cosserat rods with projective dynamics. Comput Graph Forum. 2018;37:137–147.
11. Goksel O, Salcudean SE, DiMaio SP. 3d simulation of needle-tissue interaction with application to prostate brachytherapy. Comput Aid Surg. 2006;11:279–288.
12. Chentanez N, Alterovitz R, Ritchie D, et al. Interactive simulation of surgical needle insertion and steering. ACM SIGGRAPH 2009 papers. New York, NY: Association for Computing Machinery, 2009; p. 1–10.
13. Qi D, Panneerselvam K, Ahn W, Arikatla V, Enquobahrie A, De S. Virtual interactive suturing for the fundamentals of laparoscopic surgery (fls). J Biomed Inform. 2017;75:48–62.

14. Xu L, Liu Q. Real-time inextensible surgical thread simulation. Int J Comput Assist Radiol Surg. 2018;13:1019–1035.
15. Hu Y, Zhou Q, Gao X, Jacobson A, Zorin D, Panozzo D. Tetrahedral meshing in the wild. ACM Trans Graph. 2018;37:60–61.
16. Deul C, Kugelstadt T, Weiler M, Bender J. Direct position-based solver for stiff rods. Comput Graph Forum. 2018;37(6):313–324.

AUTHOR BIOGRAPHIES

Peng Yu is a PhD candidate in the School of Computer Science, Beihang University, China. In 2015, He obtained his BSc degree in School of Internet of Things, Wuhan University of Technology. His research interests include physics-based animation, human-computer interaction and virtual surgery.

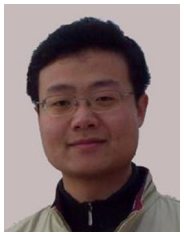

Junjun Pan received both B.Sc. and M.Sc degree in School of Computer Science, Northwestern Polytechnical University, China. In 2006, he studied in National Centre for Computer Animation (NCCA), Bournemouth University, UK as PhD candidate with full scholarship. In 2010, he received the PhD degree and worked in NCCA as Postdoctoral Research Fellow. From 2012 to 2013, he worked as a Research Associate in Center for Modeling, Simulation and Imaging in Medicine, Rensselaer Polytechnic Institute, USA. In November 2013, he was appointed as Associate Professor in School of Computer Science, Beihang University, China. His research interests include virtual surgery and computer animation.

Hong Qin is a full professor of Computer Science in the Department of Computer Science at Stony Brook University (SUNY). He received his BS and his MS in Computer Science from Peking University, China. He received his PhD in Computer Science from the University of Toronto. Currently, he serves as an associate editor for The Visual Computer, Graphical Models, and Journal of Computer Science and Technology. His research interests include geometric and solid modeling, graphics, physics-based modeling and simulation, computer aided geometric design, human–computer interaction, visualization, and scientific computing.

Aimin Hao is a professor in the Computer Science School and the Associate Director of the State Key Laboratory of Virtual Reality Technology and Systems at Beihang University. He got his BS, MS, and PhD in Computer Science at Beihang University. His research interests are on virtual reality, computer simulation, computer graphics, geometric modeling, image processing, and computer vision.

Haipeng Wang is the Chief physician in Neurology, Director of the Science and Education Department of Beijing Aerospace General Hospital. He graduated and got the master degree of Neurology from Inner Mongolia Medical University. And now he also is the adjunct professor of Xiangya Medical College, Central South University. Specialty: He is good at the clinical diagnosis and treatment of cerebrovascular diseases, neurodegenerative diseases (memory disorders, Parkinson's disease), peripheral neuropathy, sleep disorders, headache and dizziness.

How to cite this article: Yu P, Pan J, Qin H, Hao A, Wang H. Real-time suturing simulation for virtual reality medical training. *Comput Anim Virtual Worlds*. 2020;e1940. https://doi.org/10.1002/cav.1940